

# Flavour asymmetry of antiquarks in nucleon and nucleus

WenHao Ma,<sup>1</sup> Siqi Yang,<sup>1,\*</sup> MingZhe Xie,<sup>1</sup> Minghui Liu,<sup>1</sup> Liang Han,<sup>1</sup> and C.-P. Yuan<sup>2</sup>

<sup>1</sup>*Department of Modern Physics, University of Science and Technology of China, Jinzhai Road 96, Hefei, Anhui 230026, China*

<sup>2</sup>*Department of Physics and Astronomy, Michigan State University, East Lansing, MI 48823, USA*

Over the years, comprehensive experiments have shown a fact that the nucleons, such as the proton and neutron, are formed by not only the “valence” up and down quarks which were thought to comprise the nucleons in a simple constituent picture, but also “sea” quarks which can be any other flavour. However, it is still unknown how sea quarks are generated inside the nucleons. Since 1990s, measurements on high energy deuterons (formed by a proton and a neutron) indicated that the anti-down quark contribution was higher than the anti-up quark in the proton, based on the assumptions of the proton-neutron isospin symmetry and a small nuclear effect of the deuteron. Henceforth, sea quarks are considered to be generated via some flavour-asymmetrical mechanisms. Here we report an analysis on a series of new measurements from pure proton interactions which are free from those assumptions, unexpectedly showing that the anti-down quark component is rather consistent with the anti-up quark. It appears to be evidence that the previously observed asymmetry was caused by an unknown nuclear effect in the deuteron, rather than by a difference between antiquarks. We anticipate this work to be an essential new discovery and a motivation for studying nuclear structure, both experimentally and theoretically, at high energy scales, as it now appears fundamentally different from our understanding established in the past.

## INTRODUCTION AND CONCLUSION

In the simple picture of the constituent model established about sixty years ago, the proton, as one important nucleon building up the material world, is comprised of two up ( $u$ ) quarks and one down ( $d$ ) quark. They are bonded by the strong forces described by the quantum chromodynamics (QCD). However, when the energy of the proton-involved interactions is high enough that the protons are believed to break into pieces, the fragments knocked out from the protons are found to be not only the “valence”  $u$  and  $d$  quarks, but also “sea” quarks which can be any other flavour, including even antiquarks. The fundamental mechanism of how sea quarks generate inside the proton remains as a puzzle. At beginning, the anti-down ( $\bar{d}$ ) and anti-up ( $\bar{u}$ ) quarks were expected to have similar distributions in the proton, as the perturbative QCD predicts a symmetrical generation of  $\bar{d}$  and  $\bar{u}$  from the gluon splitting at high energy scale where the difference between their masses can be ignored. Unexpectedly, the distribution of  $\bar{d}(x)$  as a function of the momentum fraction  $x$  was found to be significantly higher than  $\bar{u}(x)$  from a series of experiments since 1990s [1–5], known as the SU(2) flavour asymmetry of the light quark sea. These data provide strong evidence for a non-symmetrical sea quark generation mechanism and have become the most important constraints on antiquarks in proton structure studies [6–8]. Based on these measurements, various models have been developed, trying to explain the asymmetry as a non-perturbative effect [9–15].

Although flavour asymmetry pertains specifically to sea quarks in the proton, directly measuring  $\bar{d}(x)$  and  $\bar{u}(x)$  from proton interactions has proven rather difficult. This is because these antiquarks always mix in the ini-

tial state, producing similar final states that are indistinguishable. Therefore, all those measurements mentioned above were performed with deuterons. For example, in Fermilab’s NuSea and SeaQuest experiments [1, 2], and CERN’s NA51 [3] experiment, protons are accelerated and directed to hit hydrogen and deuteron targets. The cross sections of the proton-to-hydrogen ( $\sigma_{pH}$ ) and proton-to-deuteron ( $\sigma_{pD}$ ) interactions are measured and compared with each other. Based on the assumptions of a small nuclear effect that a deuteron can be treated simply as the sum of a proton ( $p$ ) and a neutron ( $n$ ), and the isospin symmetry that the quark distributions in the proton and the neutron can be related as  $u_p = d_n$ ,  $d_p = u_n$ ,  $\bar{u}_p = \bar{d}_n$ , and  $\bar{d}_p = \bar{u}_n$ , the ratio of the antiquark distributions can be measured as  $\bar{d}/\bar{u} \approx \sigma_{pD}/\sigma_{pH} - 1$ . Other measurements, such as NMC [4] and HERMES [5], were based on lepton beams instead of proton beam, but still used deuteron target. Thus, they also assumed a small nuclear effect of deuteron. These assumptions are widely taken at low energy scales, where nuclei are nearly stationary, and are also used in nucleon structure studies at high energy scales. However, nuclear structure may differ from the understanding established in low-energy scenarios: at high energies, relativistic effects can spatially compress a nucleus, introducing unknown impacts on its observed structure. As will be discussed in detail later, this high-energy nuclear structure has never been experimentally verified.

In this article, we report a determination of the  $\bar{d}(x)$ -to- $\bar{u}(x)$  ratio at  $x \sim 0.1$ , using experimental data from pure proton interactions. This is free from the assumptions taken in the deuteron measurements. The major constraint on  $\bar{d}/\bar{u}$  comes from a series of novel measurements at the proton-(anti)proton colliders in recent years, which can decouple the contributions of different quark

flavours and reveal the information of their relative ratio [16–18]. It is achieved from the Drell-Yan process of  $hh(q\bar{q}) \rightarrow Z/\gamma^* \rightarrow \ell^+\ell^-$ , where a pair of quark and antiquark arise from the hadron collision ( $hh$ ), and annihilate into a lepton pair ( $\ell^+\ell^-$ ). The Drell-Yan process is famous for its spatial symmetry breaking at the pole region of the  $Z$  boson mass around 90 GeV, which is a unique feature of the weak force. Particularly, the cross section of the forward events, which are defined as the outgoing lepton ( $\ell^-$ ) directing to the hemisphere same as the incoming quark ( $q$ ), is different from that of the backward events, defined as  $\ell^-$  pointing to the opposite direction of  $q$ . Such forward-backward asymmetry depends on the flavour of the quarks coupled with the  $Z$  boson, and can be precisely predicted in the electroweak theory, thus can be used to separate the contributions from the up and down (anti-)quarks. As discussed in Ref. [16], the following ratios can be extracted from the forward-backward asymmetry in the proton-proton collisions and proton-antiproton collisions, respectively:

$$\begin{aligned} R_{pp} &= \frac{d(x_1)\bar{d}(x_2) - \bar{d}(x_1)d(x_2)}{u(x_1)\bar{u}(x_2) - \bar{u}(x_1)u(x_2)} \times \mathcal{N}_{EW} \\ R_{p\bar{p}} &= \frac{d(x_1)d(x_2) - \bar{d}(x_1)\bar{d}(x_2)}{u(x_1)u(x_2) - \bar{u}(x_1)\bar{u}(x_2)} \times \mathcal{N}_{EW} \end{aligned} \quad (1)$$

where  $x_1 > x_2$  are the momentum fractions of the two quarks in the initial state.  $\mathcal{N}_{EW}$  is a normalization factor contributed by the hard scattering processes involving  $q-\bar{q}-Z/\gamma^*$  couplings, which is precisely known from the higher order calculations of the electroweak theory. Contributions from other quarks, such as the strange ( $s\bar{s}$ ), charm ( $c\bar{c}$ ) and bottom ( $b\bar{b}$ ), are nearly cancelled, because the distributions of these quarks are almost equal to their corresponding antiquarks ( $s(x) \approx \bar{s}(x)$ ,  $c(x) \approx \bar{c}(x)$ ,  $b(x) \approx \bar{b}(x)$ ) [19], so that no “spatial direction” can be defined.

The  $R$  parameter has been subsequently measured by the D0 collaboration at the Fermilab’s Tevatron [17], which is a proton-antiproton collider with 1.96 TeV colliding energy, and from the proton-proton data collected by the CMS detector at the CERN’s Large Hadron Collider (LHC) at 8 TeV [18]. Due to the high beam energy, the dilepton system of the Drell-Yan process is highly boosted, giving  $x_1$  around 0.1, and  $x_2$  of  $\mathcal{O}(0.01)$  or even smaller. At such a small  $x_2$  region, distributions of light quarks are dominated by the perturbative QCD contributions, so that are comparable. Therefore,  $R_{pp}$  and  $R_{p\bar{p}}$  can be approximately written as:

$$\begin{aligned} R_{pp,p\bar{p}} &\approx \frac{d(x_1) - \bar{d}(x_1)}{u(x_1) - \bar{u}(x_1)} \times \mathcal{N}_{EW} \\ &= \frac{d(x_1) + \bar{d}(x_1) - 2\bar{d}(x_1)}{u(x_1) + \bar{u}(x_1) - 2\bar{u}(x_1)} \times \mathcal{N}_{EW}, \end{aligned} \quad (2)$$

where  $u(x_2)$ ,  $\bar{u}(x_2)$ ,  $d(x_2)$  and  $\bar{d}(x_2)$  are roughly cancelled in the ratio.  $u + \bar{u}$  and  $d + \bar{d}$  can be sufficiently constrained by comprehensive measurements of the

electron-proton deep inelastic scattering (DIS) experiments, such as HERA [20]. Thereupon, the antiquark ratio of  $\bar{d}(x)/\bar{u}(x)$  can be determined by analyzing the observed  $R$  parameter together with a group of previously performed measurements of proton-interactions, including lepton-proton DIS data from HERA and BCDMS, the proton-proton collision data from the CERN’s Large Hadron Collider (LHC), the proton-antiproton collision data from the Fermilab’s Tevatron, and the proton-hydrogen target data from the Fermilab’s E866 (NuSea). These data, as summarized in Ref. [21], are selected from the CTEQ-TEA global analysis of the proton structure, with all the nucleus-based experiments excluded. The only exception is the neutrino-iron DIS data from the NuTeV collaboration [22], which specifically constrains the strange quark distribution. We include this data to avoid potential bias in the  $\bar{d}(x)/\bar{u}(x)$  ratio that could arise from an unconstrained  $s(x)$  distribution. We have verified that including or excluding the NuTeV dataset produces only a minor numerical difference in the  $\bar{d}(x)/\bar{u}(x)$  ratio. These previously measured data do not provide direct constraint on  $\bar{d}/\bar{u}$ , but they are important for accounting for other quark and gluon contributions and higher order QCD corrections. The strategy of this analysis follows the CT18 global analysis of the proton structure [6] (but not exactly the same), in which the distributions of quarks are factorized and determined using the Hessian method [23]. To fully account for the proton’s valence quark number sum rule and momentum sum rule, we fit the distributions of all quark flavours across the entire momentum fraction range ( $x$  in  $[0, 1]$ ) using the data, although this work focuses on the  $\bar{d}(x)/\bar{u}(x)$  ratio at  $x \sim 0.1$ . Details of the analysis procedure, which has been specifically modified for this study to differ slightly from the CT18 strategy, will be presented in the next section.

For comparison, a analogous study is conducted by analyzing deuteron data from NuSea and SeaQuest, alongside proton-interaction measurements (without the  $R$ -parameter measurements), using the same methodology. This study still assumes isospin symmetry between the proton and neutron, while neglecting the deuteron’s nuclear effect. For simplicity, the NA51 [3], NMC [4] and HERMES [5] results are not used in this study, as they provide similar information and experimental conclusion, but are less sensitive. The ratios of  $\bar{d}(x)/\bar{u}(x)$  as a function of  $x$ , obtained from individual fits using either the pure proton data or the deuteron data, are demonstrated in Fig. 1. As discussed, the NuSea and SeaQuest data lead to a  $\bar{d}(x)/\bar{u}(x)$  greater than unity, indicating an asymmetry in the light quark sea of the proton. However, the pure proton data reveals the antiquark ratio to be close to unity, which is very different from the deuteron results. In Fig. 2, predictions from the two analyses are compared with the measured values of the original experimental observables, i.e. the  $R$  param-

eter and  $\sigma(pD)/(2\sigma(pH))$ . As shown, the predictions are consistent with the corresponding data which are included in the analysis. However, deviations emerge when the predictions are compared with the other dataset which are not included in the fits. As a consistency check, we performed an additional analysis of pure proton data by tripling the statistical power of the input  $R$ -parameter data. As shown in the figure, the predictions from this new analysis are more consistent with the measured  $R$  parameter, indicating that the conclusions of our original analysis are not driven by random fluctuations. This study is included solely as a sensitivity check, whereas the distributions in Fig. 1, which represent the main conclusion of this article, are presented without enhancing the data power.

The result from the pure proton interaction measurements on the antiquark ratio is of importance to the nuclear structure study. It indicates that the previous asymmetry observed from deuteron measurements could possibly be caused by some unknown nuclear effects at the corresponding energy scales. A series of measurements has been performed to investigate nuclear effects at high energies. For example, the European Muon Collaboration (EMC) had measured the ratio of the electron-iron DIS cross sections to the electron-deuteron DIS cross section, which were found to be inconsistent with the ratios of the numbers of nucleons in iron and deuteron [24]. Later, similar measurements were performed by the Jefferson lab with more nuclei included, such as carbon, tritium, helium and beryllium, and gave similar conclusions [25, 26]. The inconsistency, known as the EMC effect, has become the most important experimental evidence that the high energy nuclear structure could be different from the simple picture of bonded nucleons with small correlations. However, these experiments observe the relative difference between heavy nuclei and deuteron, whereas the analysis presented in this work probes the intrinsic (absolute) nuclear effect of the deuteron itself. Besides, in the electron-nucleus DIS measurements, the physical interactions are dominated by the contributions of the valence quarks, i.e.  $u$  and  $d$ , while this work focuses on the antiquarks. Corrections arising from potential nuclear effects may differ significantly between valence and sea quarks, as valence quark distributions dominate over sea quark contributions at  $x \sim 0.1$ . In conclusion, the discrepancy between the pure proton measurements and the deuteron data regarding the  $\bar{d}/\bar{u}$  ratio may indicate a significant nuclear effect of the deuteron which has never been directly observed before. Furthermore, On the other hand, when compared to existing experimental results, this work suggested the potential presence of previously unrecognized nuclear effects in the deuteron. To develop a more comprehensive understanding of nuclear structure, new measurements, particularly those targeting valence quark-dominated DIS and sea quark-dominated Drell-Yan processes, are urgently

needed.

This work is also crucial for the study of nucleon structure. In modern global analysis of proton structure [6–8], a wide range of nuclear data, particularly from targets such as deuteron, iron, copper and lead, is used to provide constraints, especially in the large- $x$  region. As this article already demonstrates the potential inconsistency between nucleus and proton data, it would be important to perform the global analysis of the proton structure from pure proton interactions, such as the electron-proton DIS and proton-(anti)proton Drell-Yan, jet and top quark data. In the short term, a novel global analysis excluding nuclear data would provide a hint. However, in the long run, new measurements of proton interactions, such as the proton-proton collisions at the LHC, are needed to obtain (anti)quark-related information, allowing the replacement of legacy DIS data derived from nuclei.

## GLOBAL ANALYSIS

In the study of high-energy particle collisions, the internal structure of protons and neutrons, which is the fundamental building blocks of matter, is described by Parton Distribution Functions (PDFs). These functions quantify the probability of finding a parton (a quark or gluon) that carries a specific fraction ( $x$ ) of the parent hadron's momentum. The flavour structure of PDFs is defined by distinct contributions from various quark flavours (up, down, strange, charm, bottom) and gluons. This structure is critical for accurately modeling processes in high-energy physics, as different processes exhibit sensitivity to different combinations of these distributions. In this work, we closely adopt the methodology employed by the CTEQ-TEA collaboration for PDF extraction [6]. The core of the CTEQ-TEA PDF fitting procedure relies on a set of polynomial parameterization forms, which are initially postulated at an energy scale ( $Q_0$ ) of approximately 1 GeV. These parameterization are specifically designed to describe the PDFs of various parton flavours within the proton with high accuracy. At any arbitrary high-energy scale ( $Q$ ), the PDFs are evolved using the Dokshitzer-Gribov-Lipatov-Altarelli-Parisi (DGLAP) evolution equations, leveraging the nonperturbative input PDFs determined at the  $Q_0$  scale.

In this work, the nonperturbative contributions to the PDFs of the (anti)quarks and gluons inside the proton are parameterized at  $Q_0 = 1.3$  GeV. Below, we detail a nominal set of PDFs studied in this work. The key conclusion derived from this PDF set remains consistent across the various alternative fits we have explored. For the gluon distribution, the non-perturbative function is chosen to be:

$$\begin{aligned} g(x) &= a_0 x^{a_1-1} (1-x)^{a_2} P_a^g(y) \\ P_a^g(y) &= \sinh[a_3](1-y)^3 + \sinh[a_4]3y(1-y)^2 \\ &\quad + a_5 3y^2(1-y) + y^3, \end{aligned} \quad (3)$$

where  $y \equiv \sqrt{x}$ , and  $a_5$  is fixed as  $a_5 = (3 + 2a_1)/3$ . For valence up-quark ( $u_V$ ) and down-quark ( $d_V$ ), the non-perturbative functions are:

$$\begin{aligned} f_q(x) &= a_0 x^{a_1-1} (1-x)^{a_2} P_a^V(y) \\ P_a^V(y) &= \sinh[a_3](1-y)^4 + \sinh[a_4]4y(1-y)^3 \\ &\quad + \sinh[a_5]6y^2(1-y)^2 + \left(1 + \frac{1}{2}a_1\right)4y^3(1-y) \\ &\quad + y^4, \end{aligned} \quad (4)$$

where  $y \equiv \sqrt{x}$ . For both  $u_V$  and  $d_V$ ,  $a_0$  is fixed to yield  $\int_0^1 u_V(x)dx = 2$  and  $\int_0^1 d_V(x)dx = 1$ , respectively, as the flavour number sum rules require. We further require  $a_1^{u_V} = a_1^{d_V}$  and  $a_2^{u_V} = a_2^{d_V}$ , as done in the CT18 global analysis, to ensure that the ratio between the two valence quarks take a finite value. For the sea quarks  $\bar{u}$ ,  $\bar{d}$ , and the strangeness quark  $s (= \bar{s})$ , the non-perturbative functions are:

$$\begin{aligned} f_q(x) &= a_0 x^{a_1-1} (1-x)^{a_2} P_a^{\text{sea}}(y) \\ P_a^{\text{sea}}(y) &= (1-y)^5 + a_4 5y(1-y)^4 + a_5 10y^2(1-y)^3 \\ &\quad + a_6 10y^3(1-y)^2 + a_7 5y^4(1-y) + a_8 y^5, \end{aligned} \quad (5)$$

where  $y \equiv 1 - (1 - \sqrt{x})^{a_3}$ . In the CT18 global analysis, the shape parameters are required to have  $a_0^{\bar{u}} = a_0^{\bar{d}}$ ,  $a_1^{\bar{u}} = a_1^{\bar{d}} = a_1^s$ ,  $a_2^{\bar{u}} = a_2^{\bar{d}}$ ,  $a_3^{\bar{u}} = a_3^{\bar{d}} = a_3^s = 4$ ,  $a_4^{\bar{d}} = a_8^s = 1$ ,  $a_4^s = a_5^s$ , and  $a_6^s = a_7^s$ . Besides,  $a_0^{\bar{u}}$  and  $a_0^{\bar{d}}$  are directly given by the sum rule of  $\sum_q \int_0^1 xq(x)dx = 1$ , after the normalization of other quarks are determined. In this work,  $a_2^{\bar{u}}$  and  $a_2^{\bar{d}}$  are independent parameters, as the new measurements on  $R$  can effectively constrain the difference between up and down flavours at  $x \sim 0.1$ . To fully consider the possible shift on antiquarks,  $a_0^{\bar{d}}$  is set to be a free parameter in this work, while  $a_0^{\bar{u}}$  is still calculated according to the momentum sum rule.  $a_1^{\bar{d}}$ ,  $a_1^{\bar{u}}$  and  $a_1^s$  are also set to be independent free parameters, as changes in the large  $x$  region could possibly affect the small  $x$  PDFs via the sum rules. In general, the choice of the non-perturbative functions used in this work is the same as that used in the CT18 analysis, but with four more free parameters introduced.

The non-perturbative functions, after being evolved to the corresponding energy scales of the input data using the DGLAP equations, provide the effective distributions of quarks and gluons, which are convoluted with the hard scattering cross sections to make predictions on the experimental observables of the data. The hard scattering calculations, following the same strategy as used in the CT18 global analysis, are generally performed at the next-to-next-to-leading order (NNLO) in QCD interactions. The 32 free parameters in the non-perturbative

functions are determined by comparing the predicted values of experimental observables to the values measured in data, and requiring the minimal  $\chi^2$  defined as:

$$\chi^2(a, \lambda) = \sum_k \frac{1}{s_k^2} \left( D_k - T_k(a) - \sum_\alpha \lambda_\alpha \beta_{k\alpha} \right)^2 + \sum_\alpha \lambda_\alpha^2, \quad (6)$$

where  $D_k$  and  $T_k(a)$  are the measured value and predicted value of the  $k$ -th observable included in the analysis.  $s_k$  represents the uncertainty corresponding to  $D_k$  and which is uncorrelated with the other data points. The correlated uncertainty between  $D_\alpha$  and  $D_k$  is represented by  $\beta_{k\alpha}$ , with a nuisance parameter  $\lambda_\alpha$  introduced in the analysis. Details of the establishment of Eq. (6) is discussed in Sect. III-A of Ref. [6].

The uncertainty of the global analysis is estimated using the Hessian method. In such method, the variation of  $\chi^2$  as a function of the fitted parameters  $a$  is represented in forms of a set of orthogonal eigenvectors, of which each corresponds to an independent direction in the space of the fitted parameters. For a typical  $\chi^2$  defined as in Eq. (6), the uncertainty can be quoted as the difference between the best fitted parameter values  $a_0$  and the shifted parameter values  $a'$ , corresponding to  $\Delta\chi^2 = \chi^2(a') - \chi^2_{\min}(a_0) = 1$ . In CT18, the uncertainty was enlarged by  $\Delta\chi^2 \approx 37$  to cover potential biases in the global analysis, such as the arbitrariness of the non-perturbative function formality, and tensions between experimental results. Particularly, the potential differences in the underlying physics of the experimental measurements, such as the unknown nuclear effect being studied in this work, are ignored. In this work, we consistently use the criterion  $\Delta\chi^2 = 1$  to estimate the uncertainties associated with the determined quark and gluon distributions, which represents another difference in the analysis strategy relative to the CT18. The reason for using the original uncertainty definition of  $\Delta\chi^2 = 1$  in this work is to avoid obscuring difference in the underlying physics between the pure proton datasets and the deuteron datasets.

The main conclusion from this work, the ratio of  $\bar{d}(x)/\bar{u}(x)$ , is already demonstrated in Fig. 1. To provide additional context for the analysis, we also present, in Fig. 3, the ratios of the distributions of other quark flavours and the gluon to the corresponding predictions from the CT18NNLO PDF sets. For  $u(x)$ ,  $d(x)$ ,  $\bar{u}(x)$  and  $\bar{d}(x)$ , the deuteron data analysis yields results that are more consistent with the CT18 predictions. This consistency arises because the deuteron data of NuSea was included as a key constraint in the CT18 analysis. Notably, in the proton data analysis, our results yield distributions that differ substantially from those of CT18. This is expected, as the novel measurements of the  $R$  parameters (which we incorporate here) were not available at the time of the CT18 analysis. For  $s(x) = \bar{s}(x)$  and  $g(x)$ , the two analyses in this work

yield similar distributions, as neither the  $R$ -parameter measurements nor the deuteron data provides sufficient constraints on these flavours. Instead, they are primarily determined by other experimental data included in the PDF global analysis. Furthermore, the distribution of charm quark,  $c(x) = \bar{c}(x)$ , is also consistent between the two analyses, as the charm quarks are taken to be perturbatively generated in this analysis.

## ACKNOWLEDGEMENT

This work was supported by the National Natural Science Foundation of China under Grant No. 12061141005. This work was also supported by the U. S. National Science Foundation under Grant No. PHY-2310291. We thank Dr. Yang Li from the University of Science and Technology of China and our CTEQ-TEA colleagues for many helpful discussions.

---

\* Electronic address: [yangsq@ustc.edu.cn](mailto:yangsq@ustc.edu.cn)

- [1] R. S. Towell *et al.* (NuSea Collaboration), Improved measurement of the  $\bar{d}/\bar{u}$  asymmetry in the nucleon sea, *Phys. Rev. D* **64**, 052002 (2001).
- [2] J. Dove *et al.* (SeaQuest Collaboration), The asymmetry of antimatter in the proton, *Nature* **590**, 561 (2021),
- [3] A. Baldit *et al.* (NA51 Collaboration), Study of the isospin symmetry breaking in the light quark sea of the nucleon from the Drell-Yan process, *Phys. Lett. B* **332**, 244 (1994).
- [4] M. Arneodo **et al.** (New Muon Collaboration), Measurement of the proton and deuteron structure functions,  $F_2^p$  and  $F_2^d$ , and of the ratio  $\sigma_L/\sigma_T$ , *Nucl. Phys. B* **483**, 3 (1997).
- [5] K. Ackerstaff *et al.* (HERMES Collaboration), The Flavor asymmetry of the light quark sea from semiinclusive deep inelastic scattering, *Phys. Rev. Lett.* **81**, 5519 (1998).
- [6] Tie-Jiun Hou *et al.*, New CTEQ global analysis of quantum chromodynamics with high-precision data from LHC, *Phys. Rev. D* **103**, 014013 (2021).
- [7] S. Bailey, T. Cridge, L. A. Harland-Lang, A. D. Martin, R. S. Thorne, Parton distributions from LHC, HERA, Tevatron and fixed target data: MSHT20 PDFs, *Eur. Phys. J. C* **81**, 341 (2021).
- [8] R. D. Ball *et al.* (NNPDF), The path to proton structure at 1% accuracy, *Eur. Phys. J. C* **82**, 428 (2022).
- [9] J. Alwall, G. Ingelman, Quark asymmetries in the proton from a model for parton densities, *Phys. Rev. D* **71**, 094015 (2005).
- [10] Y. Ding, R.-G. Xu, B.-Q. Ma, Effect of asymmetric strange-antistrange sea to the NuTeV anomaly, *Phys. Lett. B* **607**, 101 (2005).
- [11] Y. Ding, R.-G. Xu, B.-Q. Ma, Nucleon sea in the effective chiral quark model, *Phys. Rev. D* **71**, 094014 (2005).
- [12] H. Song, X. Zhang, B.-Q. Ma, Light flavor asymmetry of nucleon sea, *Eur. Phys. J. C* **71**, 1542 (2011).
- [13] M. Wakamatsu, Light flavor sea quark distributions in the nucleon in the SU(3) chiral quark soliton model. 1. Phenomenological predictions, *Phys. Rev. D* **67**, 034005 (2003).
- [14] M. Wakamatsu, On the NuTeV anomaly and the asymmetry of the strange sea in the nucleon, *Phys. Rev. D* **71**, 057504 (2005).
- [15] M. Wakamatsu, Transverse momentum distributions of quarks in the nucleon from the Chiral Quark Soliton Model, *Phys. Rev. D* **79**, 094028 (2009).
- [16] Siqi Yang *et al.*, Factorization of the forward-backward asymmetry and measurements of the weak mixing angle and proton structure at hadron colliders, *Phys. Rev. D* **106**, 033001 (2022).
- [17] V. M. Abazov *et al.* (D0 Collaboration), Up and down quark structure of the proton, *Phys. Rev. D* **110**, L091101 (2024).
- [18] Mingzhe Xie *et al.*, Measurement of the proton structure parameters in the forward-backward charge asymmetry, *Phys. Rev. D* **107**, 054008 (2023).
- [19] Stefano Catani, Daniel de Florian, Geman Rodrigo, and Werner Vogelsang, Perturbative generation of a strange-quark asymmetry in the nucleon, *Phys. Rev. Lett.* **93**, 152003 (2004).
- [20] H. Abramowicz *et al.* (H1 and ZEUS) Collaborations, Combination of measurements of inclusive deep inelastic  $e^\pm p$  scattering cross sections and QCD analysis of HERA data, *Eur. Phys. J. C* **75**, 580 (2015).
- [21] A. Ablat *et al.*, New results in the CTEQ-TEA global analysis of parton distributions in the nucleon, *Eur. Phys. J. Plus* **139** (2024) 12, 1063.
- [22] M. Goncharov *et al.* (NuTeV Collaboration), Precise measurement of dimuon production cross-section in  $\nu_\mu$  Fe and  $\bar{\nu}_\mu$  Fe deep inelastic scattering at the Tevatron. *Phys. Rev. D* **64**, 112006 (2001).
- [23] J. Pumplin *et al.*, Uncertainties of predictions from parton distribution functions. 2. The Hessian method, *Phys. Rev. D* **65**, 014013 (2001).
- [24] J. J. Aubertet *et al.*, The ratio of the nucleon structure functions  $F_2^N$  for iron and deuterium, *Phys. Lett. B* **123** (1983) 275-278.
- [25] J. Seely *et al.*, New measurements of the EMC effect in very light nuclei, *Phys. Rev. Lett.* **103**, 202301 (2009).
- [26] D. Abrams *et al.*, Jefferson Lab Hall A Tritium Collaboration, EMC Effect of Tritium and Helium-3 from the JLab MARATHON Experiment *Phys. Rev. Lett.* **135**, 062502 (2025).

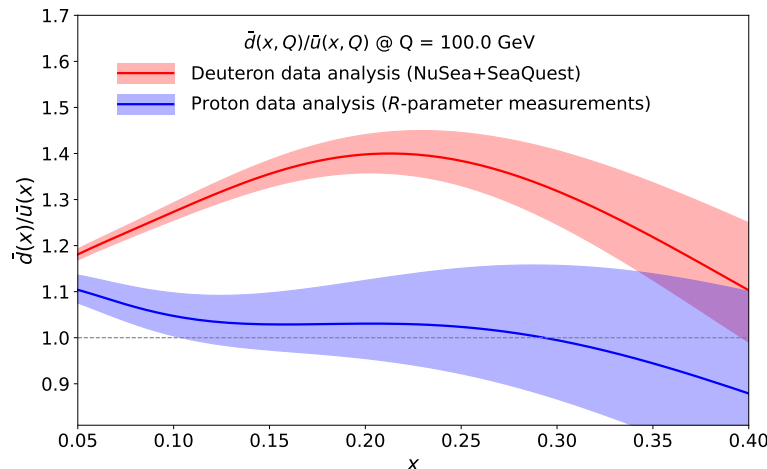
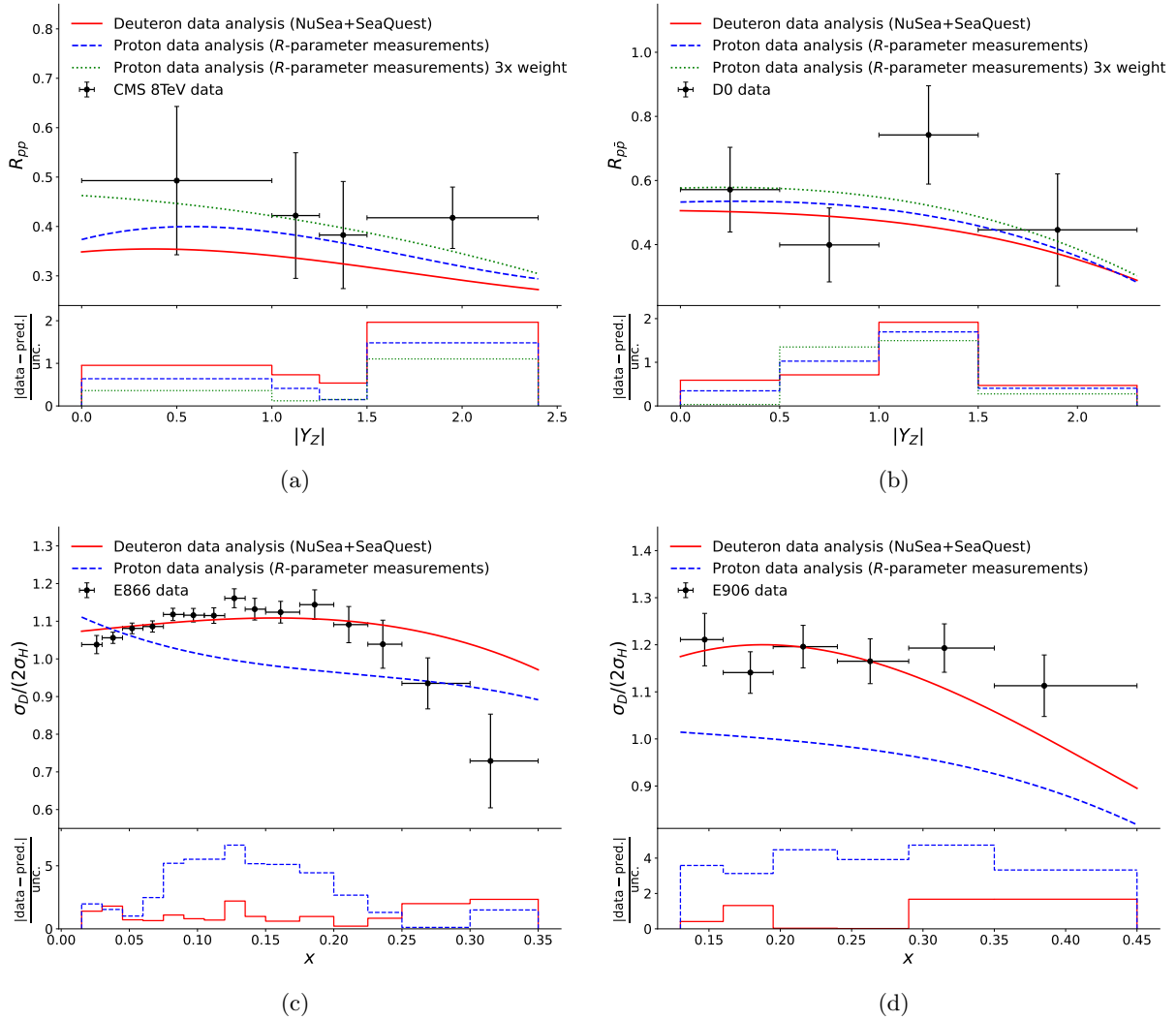
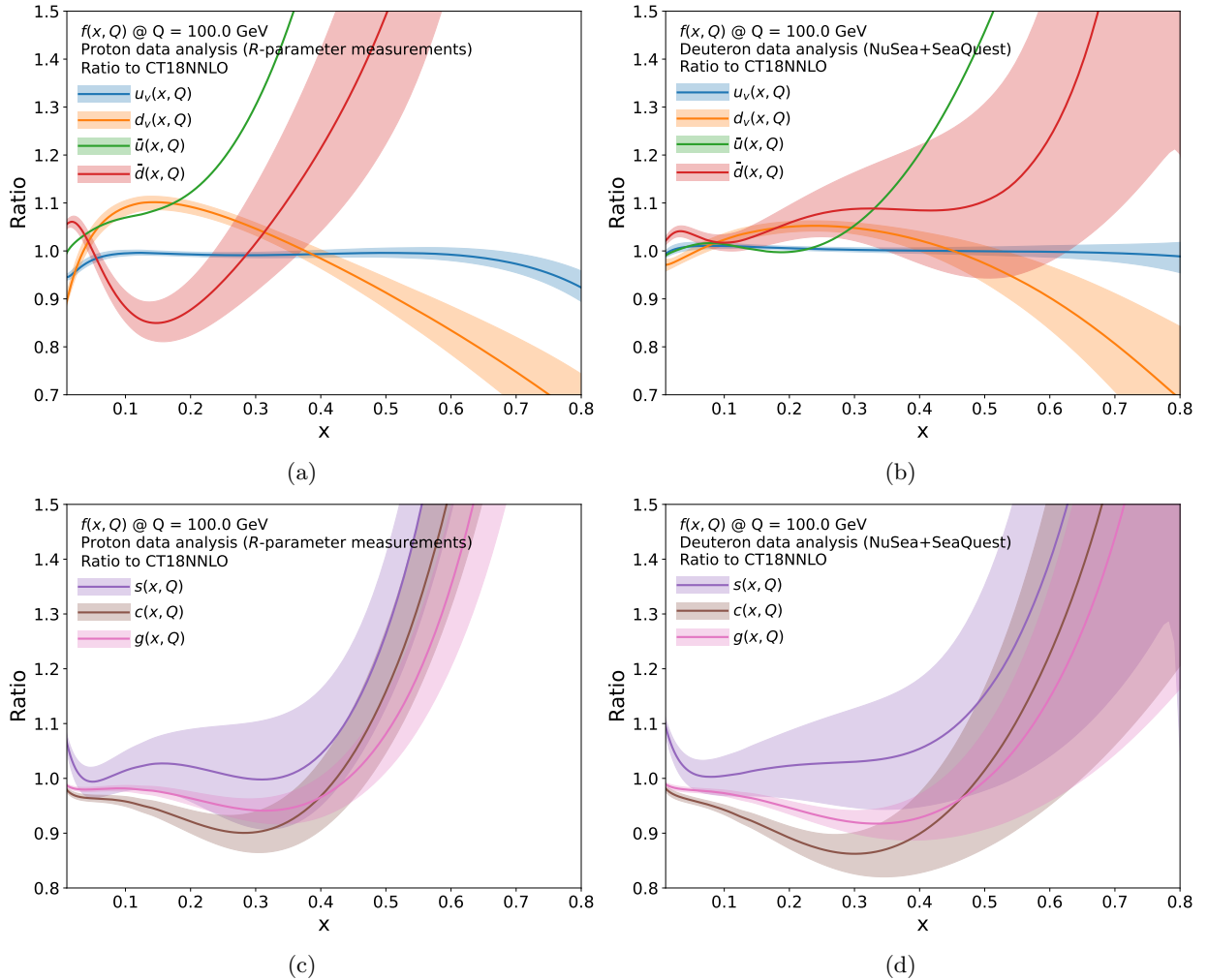


FIG. 1: **Distributions of  $\bar{d}(x)/\bar{u}(x)$ .** Distributions of  $\bar{d}(x)/\bar{u}(x)$ , obtained from two separated analyses, one using pure proton data (blue curve with uncertainty band in same colour) and another using deuteron data (red curve with uncertainty band in same colour). The proton data-based analysis incorporates experimental results from HERA, BCDMS, LHC, Tevatron, and Fermilab's E866 (specifically, only the proton-hydrogen measurement). Additionally, measurements used to determine the  $R$ -parameter are included to constrain the antiquark distributions. In contrast, the deuteron-based analysis replaces the  $R$ -parameter measurements with experimental results from the NuSea and SeaQuest collaborations. For consistency, all distributions are calculated at the energy scale of 100 GeV. The uncertainties of these distributions are estimated by taking into account both the statistical errors and experimental systematics of the measurements.



**FIG. 2: Comparison between the data and predictions.** The measured  $R$  parameters from the CMS (a) and D0 (b) data, together with the measured  $\sigma(pD)/[2\sigma(pH)]$  from the NuSea (c) and SeaQuest (d) data, are shown. The vertical error bars represent the total uncertainties, including both statistical fluctuations and experimental systematics. The corresponding theoretical predictions (in solid or dashed curves) for these observables are provided for comparison. The lower panel in each subfigure displays the uncertainty-normalized difference between the predictions and the measurements, i.e., the difference divided by the standard deviation. The  $R$  parameters are presented as a function of  $|Y_Z|$ , the rapidity of the Drell-Yan pair, while the ratio of  $\sigma(pD)/[2\sigma(pH)]$  is presented as a function of  $x$ .



**FIG. 3: Relative distributions of quarks and gluon.** The quark and gluon distributions derived from the analysis of the pure proton dataset and that of the deuteron dataset, demonstrated as the ratio with respect to the corresponding predictions from CT18NNLO PDF. For the distributions of  $u(x)$ ,  $d(x)$ ,  $\bar{u}$  and  $\bar{d}$ , the ratios are given in (a) and (b) for the proton data and the deuteron data analysis, respectively. For the distributions of  $s(x) = \bar{s}(x)$ ,  $g(x)$  and  $c(x)$ , the ratios are given in (c) and (d) for the proton data and the deuteron data analysis, respectively.